

## Chapter 3

### Flexible Dual-Band Antenna Fabricated on Silicon Suspended Parylene Membrane

In this chapter, a simple novel monopole membrane antenna was designed and fabricated on a silicon suspended parylene membrane. This parylene membrane is a flexible polymer film, it's a thin flexible substrate, which can be coated-on or peel-off from various shapes and surfaces of materials. Because of its low deposition processing temperature, it is possible to be fabricated on CMOS circuits post process with MEMS technology. The low cost, easy fabrication, easily stick-on and peel-off flexible properties of this parylene membrane makes it very attractive and convenient in any wireless portable devices such as mobile phone, RFID tag, Bluetooth and WLAN devices, even any wearable clothes...etc.

#### 3-1. Motivation

Wireless communication technology has led to many new applications of this technology in military and personal communication systems. The requirements for mobile personal communication devices and systems, such as mobile phones, personal digital assistants (PDAs), RFID, Bluetooth systems, and wireless local area networks (WLANs) are: high performance, light weight, small volume, low cost, and easily mount. Among these systems or devices, wireless links are used for

transmitting and receiving voices, images, and data; hence, antennas are not only indispensable but also play an important role in the quality of service using these wireless communication systems. The printed dual-band antenna has been studied due to this increasing demand [1]~[2]. Moreover, in some wireless applications, it might be necessary to stick the antenna on a portable device to have a radiation effect. Such as the RFID, where antennas printed on a flexible substrate are highly desirable, so that this tags can be simply attached onto any objects [3]. In addition, in order to achieve better performance as well as more functions, radio-frequency microelectromechanical systems (RF-MEMS) technology has been applied to the design and fabrication of various antennas [4]~[6].

Poly-para-xylylene (parlyene) is the generic name for members of a unique polymer series. The most used types are parlyene-n, parlyene-c and parlyene-d; each of them has slight differences in physical properties. Parlyene can be deposited conformably by chemical vapor deposition (CVD) at room temperature, so it is compatible with low-temperature microfabrication technologies such as sputtering, lithography, etching, and other commonly used processing techniques. Moreover, parlyene also has low gas permeability and is inert to many chemical agents. Owing to its excellent mechanical properties such as being stress-free and hydrophobic, parlyene is frequently used as an anti-stiction layer and structural material (cantilever beam, membrane, etc.) in micro-mechanical devices. There have been several parlyene-based MEMS devices demonstrated [7]~[9], and parlyene is also suitable for RF applications [10], particularly for RF MEMS devices, which need both good mechanical and electrical properties. Table 3-1 shows the main physical properties of parlyene [11]~[12]. With these properties, parlyene can be used as an inter-metal dielectric material, a substrate material, and an isolation/passivation layer in high-frequency circuits.

To use parylene as an antenna substrate, due to the low dielectric constant of the parylene, fewer surface waves will be excited; hence the bandwidth and radiation efficiency of the antenna will be enlarged. In addition, because of parylene's high resistivity, the RC and eddy current losses of the substrate are minimized, and the radiation efficiency of the antenna is improved. The inertness to chemicals facilitates the antenna fabrication chemical processes, and the flexibility of the substrate enables it to be easily assembled into systems.

In this study, a dual antenna was designed, the frequencies were chosen to be in the range of 2.4~2.48 GHz and 5.15~5.35 GHz. Parylene-n substrate is used due to its lowest dielectric constant and dissipation factor, and it has the highest dielectric strength among the three parylene series. This dual-band monopole antenna were designed with meander-shaped metal tracks, because this can efficiently reduce the physical dimensions of the overall antenna size while still maintaining the required electric path length. The monopole antennas were fabricated on a parylene-n membrane coated on a silicon carrier substrate. This flexible antenna membrane can be peeled off after the fabrication is completely processed. The design, simulation, and measurement results of the experimental antennas are presented in this dissertation. The advantages of these antennas are their small size, light weight, low cost, dual-band characteristic, broad bandwidth, and flexibility.

## 3-2. Design and Fabrication

### 3-2.1 Antenna Design

In this design, the folded monopole parylene membrane antenna provides two resonant paths of different lengths to achieve the desired dual-band (2.4GHz/5.2GHz) operation for Bluetooth and WLAN application. The resonant frequency of the monopole antenna is mainly determined by its physical dimensions and the dielectric constant of the substrate material. By means of the meander-shaped track design, the antenna size can be reduced without changing its resonant frequency. Dual-frequency operation was obtained by a branch-line monopole composed of two stripes resonating at two different frequencies [13]. In order to simplify and shorten the optimization design time, *IE3D software version 8* [14] was used to calculate the resonant frequencies of the designed antenna. Figure 3-1 illustrates the detailed geometry and dimensions of the designed low-profile meander antenna. The dual frequencies were chosen to be in the range of 2.4~2.48 GHz and 5.15~5.35 GHz for the two commonly used frequency bands. The dual-striped meander-shaped line's dimensions are calculated at a quarter wave length for the desired resonant frequencies. As shown in Fig. 3-1, the longer branch on the left of the meander-shaped antenna is for the resonant frequency at 2.4 GHz, while the shorter branch on the right matches the resonant frequency at 5.2 GHz. The 2D view and 3D view of the simulated antenna were shown in Fig. 3-2. The simulated  $S_{11}$  parameter was designed for the operation frequencies in the Bluetooth application. In our simulated results of radiation patterns, this antenna also exhibits omnidirectional-like radiation patterns along y-directed electric monopole placed on a finite ground plane. It is worth noting that because of the corner effects between adjacent meandered sections, the actual length of this prototype is longer than the quarter-wavelength monopole antenna. The antenna was fed from the center using a quarter-wavelength impedance transformer microstrip lines to achieve good impedance matching.

### 3-2.2 Deposition of Parylene membrane

The equipment used for parylene deposition in our study is PDS 200 (Specialty Coating Systems), as shown in Fig. 3-3. The parylene deposition process consists of three steps, as shown in Fig. 3-4. First, the parylene polymers are vaporized from the solid dimer at approximately 150 °C in the vaporizer. The second step is the pyrolysis cleavage at about 680 °C that yields the stable monomeric diradical para-xylylene. Finally, the monomers enter the deposition chamber, which was held at room temperature, and polymerize on the substrate and chamber wall. Note that the thickness of the deposited parylene depends on the weight of the parylene solid dimer that has been put in the vaporizer as the source.

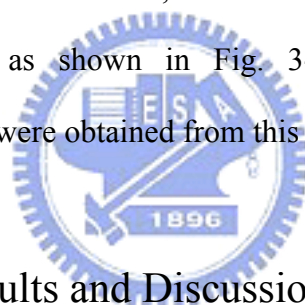
During the deposition, the substrate temperature never increases more than a few degrees above room temperature. The residual monomers were then exhausted and filtered through a cold trap by a mechanical pump. The function of the cold trap is to prevent the monomers from coating the rotor of the mechanical pump in the exhaust system.

### 3-2.3 Process of Antenna Fabrication on Parylene

The fabrication process flow of the antenna fabricated on the parylene substrate is shown in Fig. 3-5. A microsoap solution, 2% Micro-90\_(Specialty Coating Systems) solution, which has often been used as a cleaner or detergent, was first coated on a silicon substrate prior to parylene deposition to serve as a releasing agent for easy peel-off after the device is completely processed. When the substrate is coated with the soap solution, the adhesion is so low that the parylene membrane can be peeled off easily from the substrate with tweezers. After 15- $\mu\text{m}$ -thick parylene deposition, a

200-nm/100-nm-thick Cu/Ti plating seed layer was then deposited, and a 20- $\mu\text{m}$ -thick photoresist (PR), AZ 9260, which was used as the electroplating mold, was patterned using a conventional lithography process. After 20- $\mu\text{m}$ -thick copper electroplating, the PR mold was stripped by immersing the wafer in acetone, and then the seed layer was etched using diluted HF. Finally, the parylene with the fabricated copper structures was peeled off from the silicon carrier substrate. It should be noted that the silicon carrier wafer can theoretically be reused an unlimited number of times, and therefore contributes no cost to the antenna device.

In order to demonstrate the feasibility and performance of our design, the antenna was designed for application in a Bluetooth module. After peeling off the parylene membrane with the antenna on it, the antenna was successfully stucked on a portable Bluetooth dongle, as shown in Fig. 3-6. The antenna performance characteristics measurements were obtained from this module.



### 3-3. Measurement Results and Discussion

#### 3-3.1 Return Loss of Dual-band Monopole Antenna

The simulated return loss as a function of frequency was obtained using the software *IE3D version 8* to calculate the frequency response and the resonant frequencies of the designed antenna. The simulated and the measured results are compared in Fig. 3-7, which shows that the measured lower resonant band has a bandwidth of about 140 MHz, determined by 2.5 VSWR (Voltage Standing Wave Ratio), which covers the Bluetooth and WLAN 802.11b band (2.400~2.480 MHz). In addition, the measured upper resonant band has a bandwidth of about 550 MHz,

covering the 5.2 GHz (5150-5350 MHz) WLAN 802.11a, which is useful for practical applications. The measured results agree reasonably well with the simulated data. The slight difference between the simulated and measured results is probably a result of the fabricated metal thickness and dimensions deviated from the designed value due to the copper electroplating process. In addition to this, the thin adhesive tape used to stick the antenna to the Bluetooth board may have had some influence on the measured data. Although the prototype is small in dimensions, reasonable impedance and bandwidths are observed.

### 3-3.2 Antenna Radiation Characteristics

The radiation characteristics of the designed and fabricated antennas have also been measured in the x-z plane and the y-z plane. The setup for the measurement of the x-z plane radiation pattern of this membrane antenna under a far field  $R \geq 2D^2 / \lambda$  is shown in Fig. 3-8. Note that R is the distance between the horn antenna and the membrane antenna, D is the maximum length of the membrane antenna, and  $\lambda$  denotes the wavelength. The radiation patterns of the E plane and H plane were measured by the horn antenna by rotating the membrane antenna along the  $\theta$  and  $\psi$  directions. Note that E- $\theta$  denotes the radiation patterns of the E plane measured along the  $\theta$  direction and E- $\psi$  denotes the radiation patterns of the E plane measured along the  $\psi$  direction. In Figs. 3-9 and 3-10, measured radiation patterns are plotted at center operating frequencies of 2.4 and 5.2 GHz, respectively. Figures 3-9(a) and 3-9(b) show the co-polar and cross-polar radiation patterns for the E and H plane at 2.4 GHz and Figures 3-10(a) and 3-10(b) show the co-polar and cross-polar radiation patterns at 5.2 GHz. In general, it can be seen that the co-polarization radiation patterns at both 2.4 and 5.2 GHz are approximately omnidirectional and are

similar to those of a y-directed electric monopole placed on a finite ground plane. This antenna also exhibits omnidirectional-like radiation patterns in other planes. The 2.4 and 5.2 GHz-associated numerical maximum radiation gains are 0.5 and 0.9 dBi, respectively. The characteristics of this antenna satisfy simultaneously almost all the Bluetooth and WLAN application requirements.

From the above results and discussion, we can see that the characteristics of an antenna fabricated by the proposed technology can be predicted by simulation tools. Thus, the technology described in this study can be easily adopted for other applications such as RFID (Radio Frequency Identification) tag fabrication because it is inexpensive in terms of both design and fabrication, and the flexible parylene substrate makes it suitable for even wider applications.

#### 3-4. Folded Dual-Band Antenna Type



By using the same design concepts and fabrication process, another design of the flexible dual-band monopole antenna can also be accomplished, as shown in Fig. 3-11. Figure 3-12 shows the comparison between the simulated and measured return loss of this dual-band monopole antenna. The measured 2.5 VSWR return loss bandwidth for the lower frequency band is about 140 MHz, which is sufficient to cover the Bluetooth and WLAN 802.11b band (2.400~2.480MHz). As for the upper frequency band, the measured bandwidth is about 530 MHz, which is also sufficient to cover 5.2 GHz (5150-5350 MHz) WLAN 802.11a. The measurement results agree reasonably well with the simulated data. Figure 3-13 and Figure 3-14 show the measured radiation patterns at 2.4 GHz and 5.2 GHz, respectively. All the radiation characteristics have also been investigated in the x-z plane and y-z plane. A



reasonably Monopole-like and well omni-directional radiation patterns are also observed. Though the dimension of this antenna is slightly larger than the one described in section 3-2, it has better performance in bandwidth.

### 3-5. Conclusions

In this study, a dual-band monopole antenna fabricated on a parylene membrane for application to a Bluetooth module was demonstrated. Since parylene is a flexible polymer film, it can be coated on various substrates or even peeled off and used as a thin flexible substrate by itself. Due to parylene's excellent physical, mechanical and chemical properties such as low dielectric constant, high resistivity, and inertness to chemicals, it can serve as a substrate for an antenna or other kinds of RF devices. The measured results of the fabricated antennas agree very well with the simulated results, and hence the characteristics of the antenna can be well designed and accurately predicted before fabrication. We conclude that the technology presented here offers possibilities for other applications such as WLANs, mobile phones, RFID tags (as shown in Fig. 3-15) and other mobile wireless communication devices. Due to its flexibility, a flexible RFID card with low cost and high performance can be realized. The technology we described is a low-temperature process; hence, it is also suitable for complementary metal oxide semiconductor (CMOS) post-process device fabrication.

### 3-6. References

- [1] J. Y. Jan and L. C. Tseng, "Planar monopole antennas for 2.4/5.2 GHz dual-band application," in IEEE AP-S. Int. Symp. Dig., pp. 158-161, 2003.
- [2] S. H. Yeh and K. L. Wong, "Dual-Band F-shaped Monopole Antenna for 2.4GHz/5.2GHz WLAN Application," IEEE Antenna and Propagation Society International Symp., vol. 1, pp.72-75, 2002.
- [3] L. Ukkonen, L. Sydanheirno, M. Kivikoski, "A novel tag design using inverted-F antenna for radio frequency identification of metallic object," Advances in Wired and Wireless Communication, 2004 IEEE Sarnoff Symposium, April 26-27, 2004 pp.91-94.
- [4] Rhonda F. Drayton, et al, "Microstrip Patch Antennas on Micromachined Low-Index Materials," IEEE Antennas and Propagation Society International Symposium, 1995, AP-S. Digest, volume: 2, 18-23, June 1995, pp. 1220-1223.
- [5] J.-C. Chiao, "MEMS RF Devices For Antenna Applications", IEEE Microwave Conf., 2000 Asia-Pacific, 3-6, Dec. 2000, pp. 895-898.
- [6] Chang-Wook Baek, and Seunghyun Song et al, "2-D Mechanical Beam Steering Antenna Fabricated Using MEMS technology," IEEE MTT-S Digest, 2001, pp.211-214.
- [7] X. Q. Wang, Q. Lin, and Y. C. Tai, "A Parylene Micro check Valve," Proceedings of the 12<sup>th</sup> IEEE International Conference on Micro Electro Mechanical Systems (MEMS'99), Florida, U.S.A, Jan. 17-21, 1999, pp.177-182.
- [8] Pornsin-Sirirak, et al., "Flexible parylene-valved skin for adaptive flow control." Micro Electro Mechanical Systems, 2002. The Fifteenth IEEE International Conference on, 20-24 Jan. 2002, pp. 101 – 104.

- [9] Ellis Meng; Yu-Chong Tai; “A parylene mems flow sensing array.”  
TRANSDUCERS 2003, 12th International Conference on Solid-State Sensors,  
Actuators and Microsystems, 2003, Volume: 1, pp. 686 – 689.
- [10] C.-U. Huang, I-Y. Chen, H. J. H. Chen, C. F. Jou and S. R.-S. Huang, “High  
Performance Low Cost Patch Antenna Fabricated on Silicon Suspended Parylene  
Membrane”, ICEE 2004/APCOT MNT, Asia-Pacific Conf. Transducers and  
Micro-Nano Technology, 2004, Vol. 3-2, pp. 1003.
- [11] Webpage: <http://www.vp-scientific.com/index.htm>
- [12] Webpage: <http://paratronix.com/apps/techdata.asp>
- [13] T. H. Kim and D. C. Park, “CPW-fed compact monopole antenna for dual-band  
WLAN applications”, Electronics Letters, Volume 41, Issue 6, 17 March 2005,  
pp. 291 - 293.
- [14] IE3D, Zeland Software, Inc.



<i>Properties</i>	<b>Parylene-n</b>	<b>Parylene-c</b>	<b>Parylene-d</b>
<b>Surface resistivity</b> ( $\Omega$ )	$10^{13}$	$10^{14}$	$10^{16}$
<b>Dielectric constant</b> (at 1 MHz)	2.65	2.95	2.80
<b>Dissipation factor</b> (at 1 MHz)	0.0006	0.013	0.002
<b>Dielectric strength</b> (V/mile)	7000	5600	5500
<b>Tensile strength</b> (MPa)	~ 42	~ 76	~76
<b>Yield strength</b> (psi)	6100	8000	9000

Table 3-1: Main properties of parylene. (3-6. [11], [12])

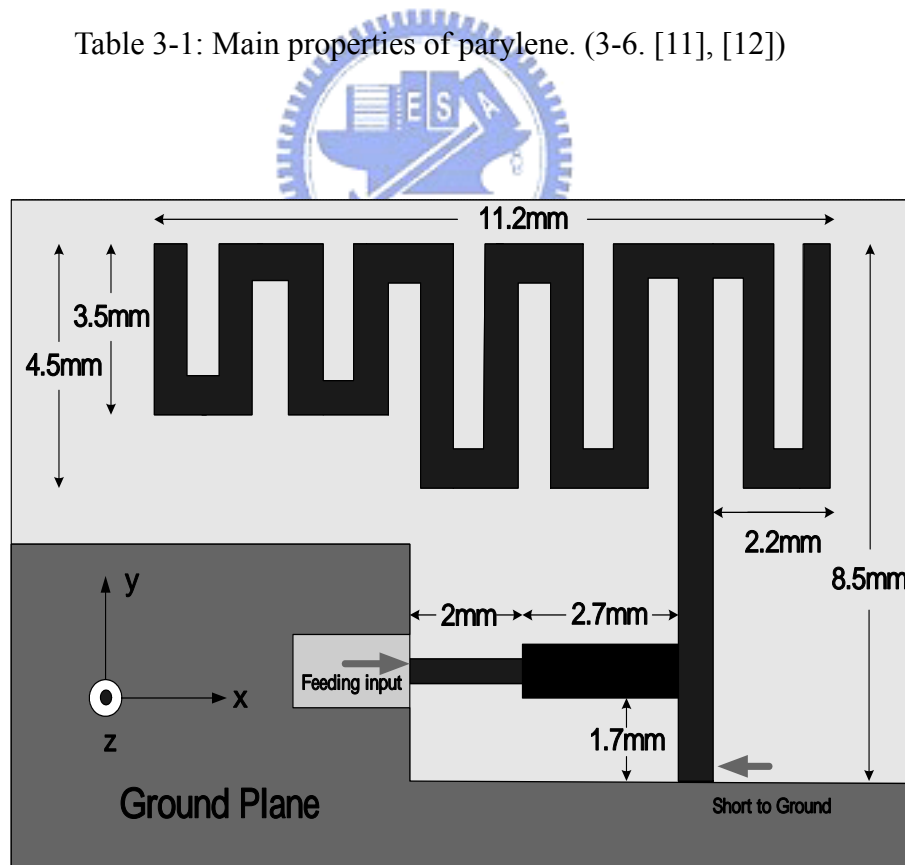
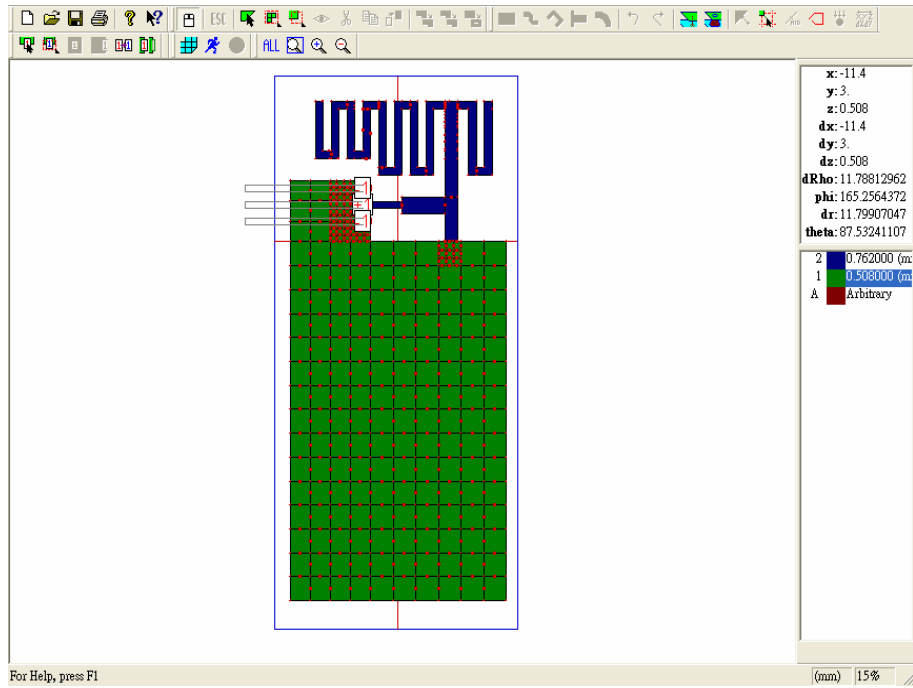
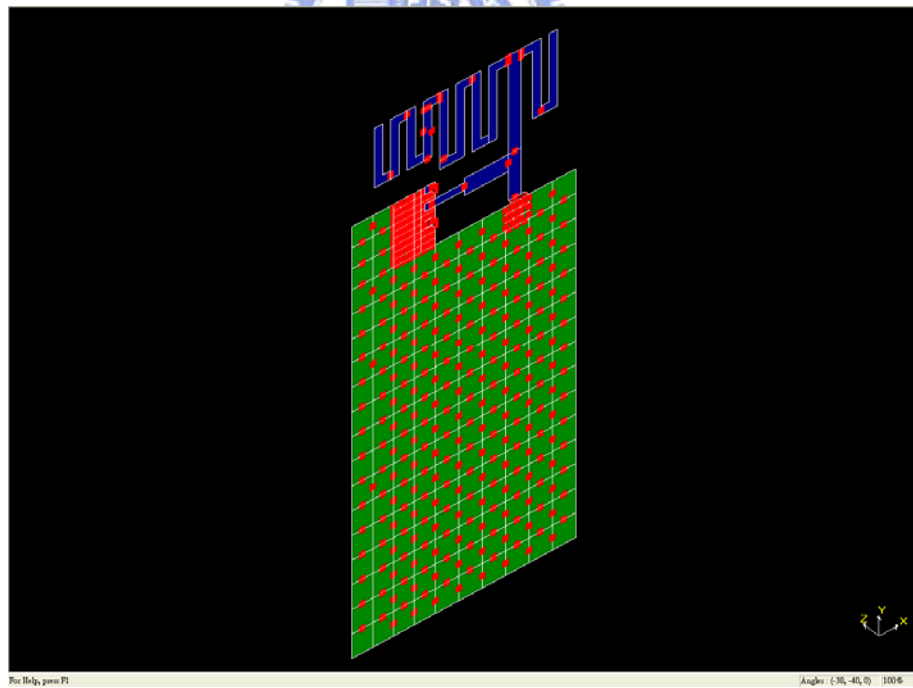


Figure 3-1: Detailed geometry and dimensions of designed dual-band meander monopole antenna.



(a)



(b)

Figure 3-2: Simulation of the dual-band monopole antenna.



Figure 3-3: Equipment for parylene deposition, PDS 200.

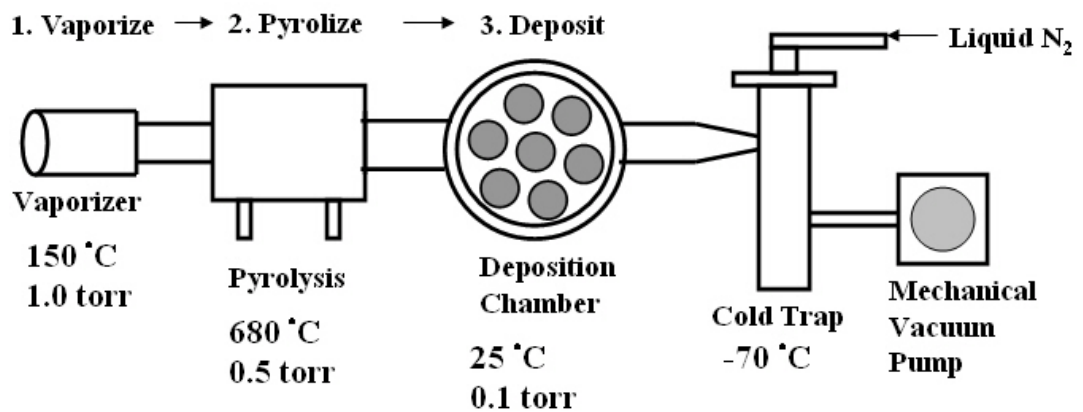
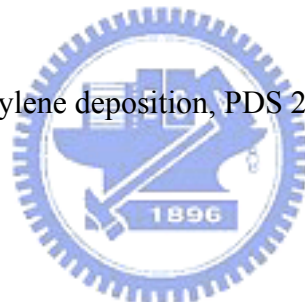


Figure 3-4: Deposition process of parylene. (3-6. [11], [12])

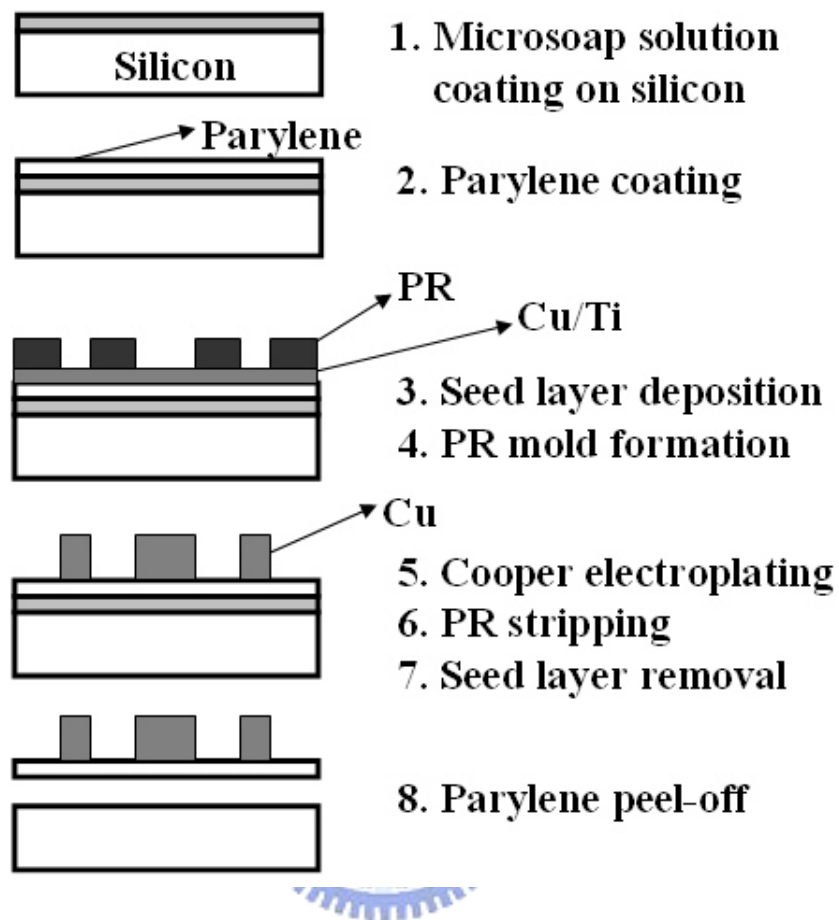


Figure 3-5: Fabrication process of designed antenna on parylene-coated silicon substrate.



(a)



(b)

Figure 3-6: Fabricated dual-band meander monopole antenna (a) before and (b) after being stacked on Bluetooth dongle.



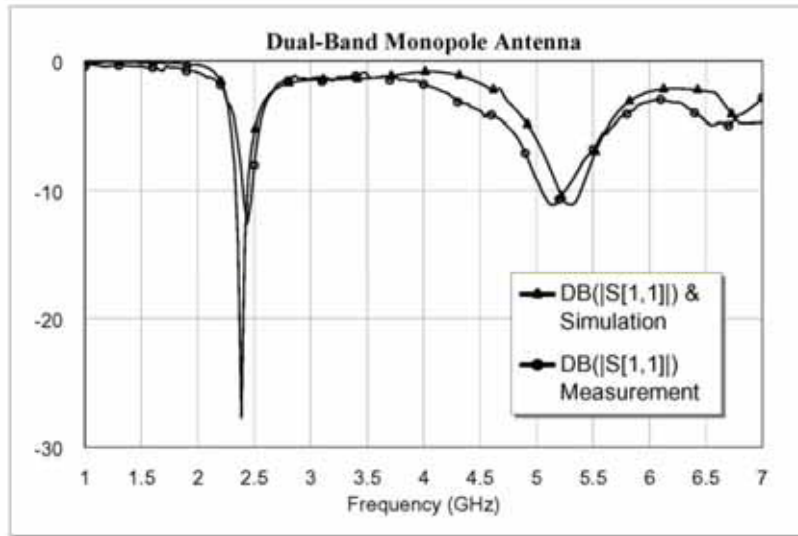


Figure 3-7: Measured and simulated return losses for the dual-band monopole antenna (2.4 and 5.2 GHz for Bluetooth and WLAN).

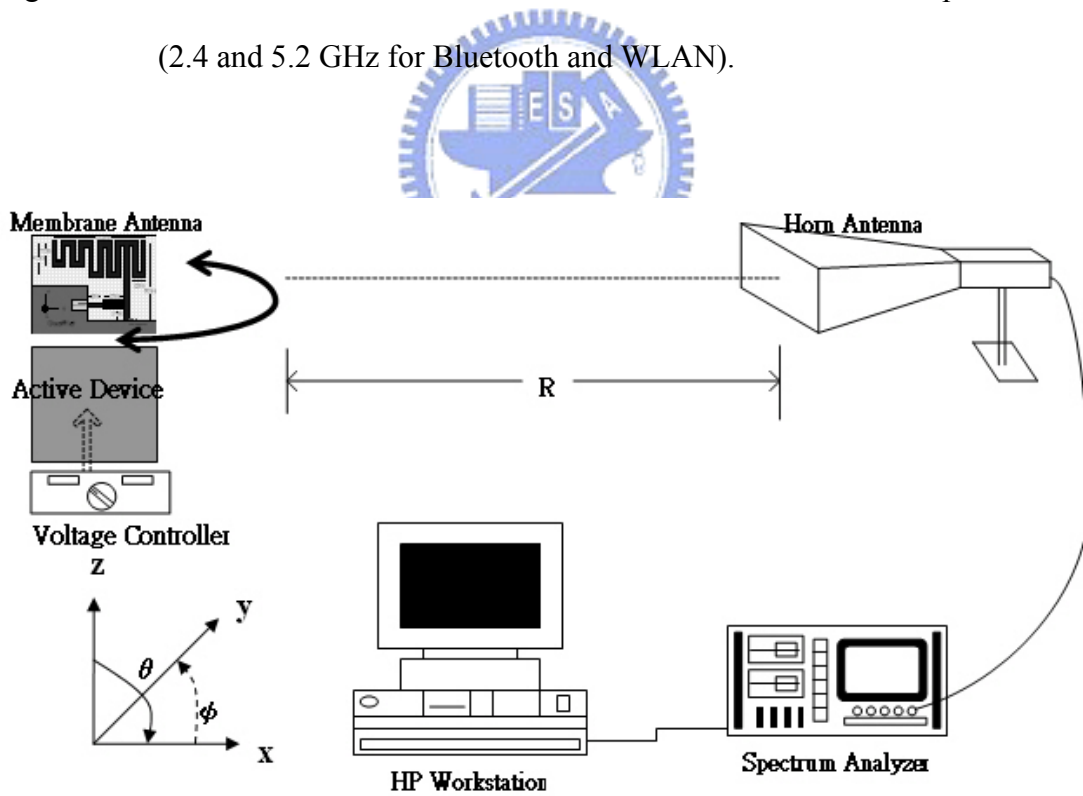
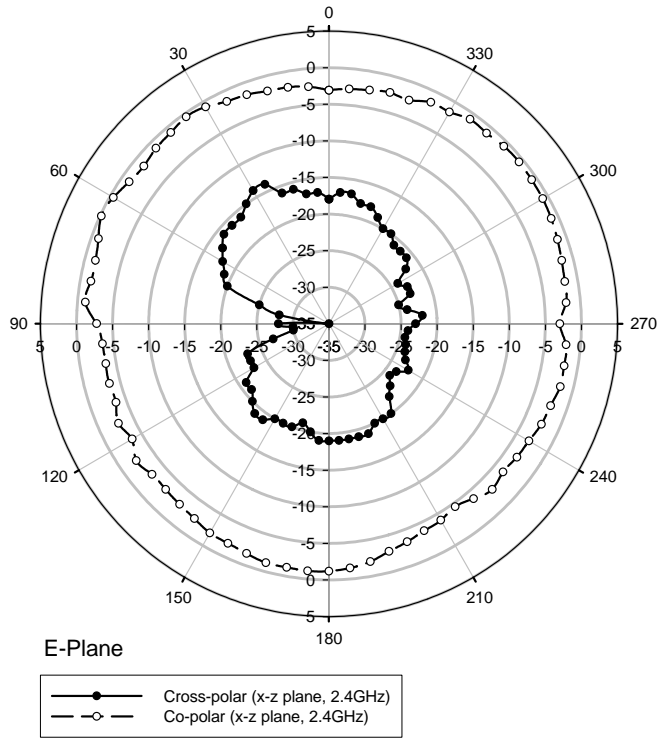
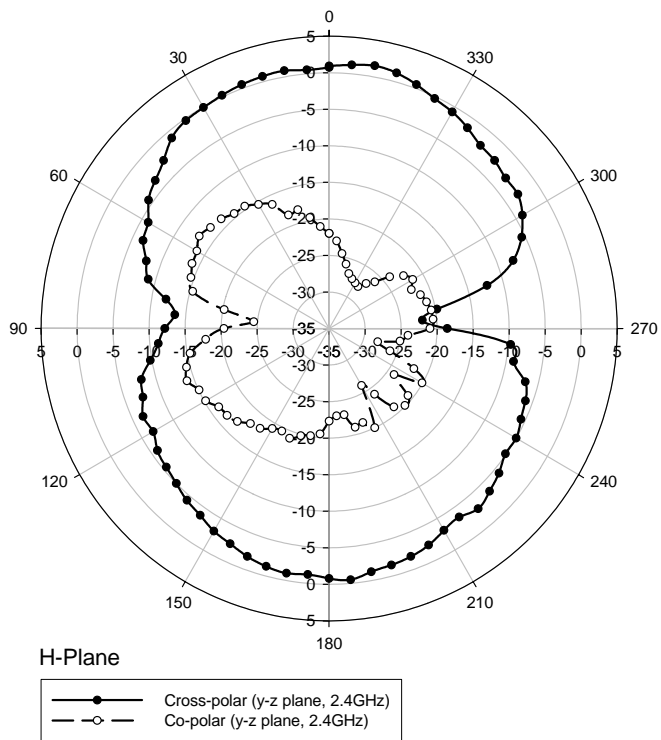


Figure 3-8: x-z plane radiation pattern measurement setup of MEMS membrane monopole antenna under far-field conditions.

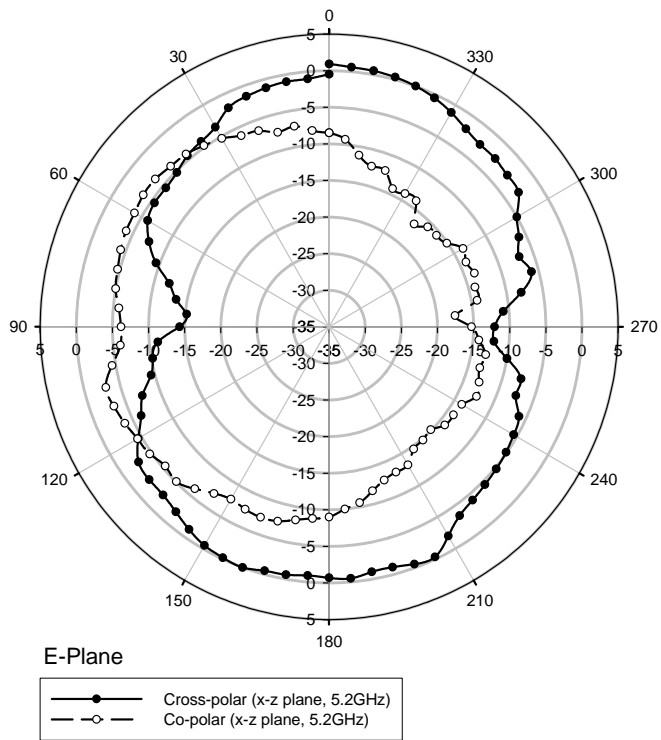


(a)

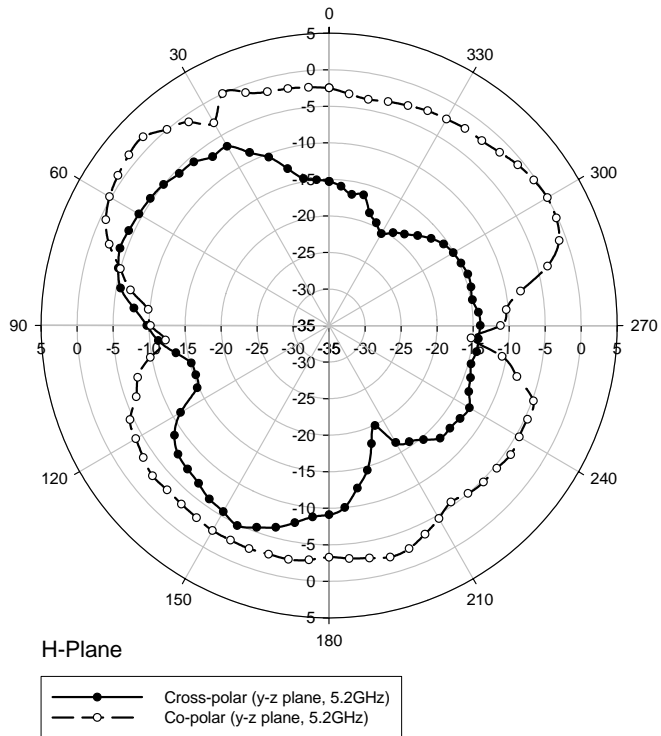


(b)

Figure 3-9: Measured x-z and y-z plane radiation patterns for the proposed antenna at 2.4GHz.



(a)



(b)

Figure 3-10: Measured x-z and y-z plane radiation patterns for the proposed antenna at 5.2GHz.

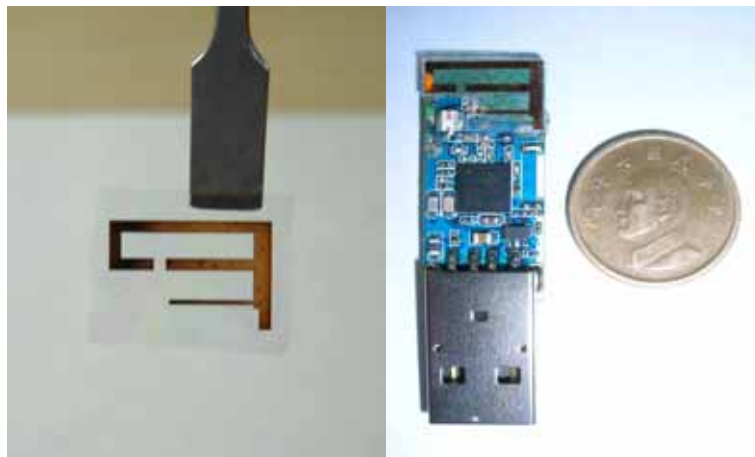
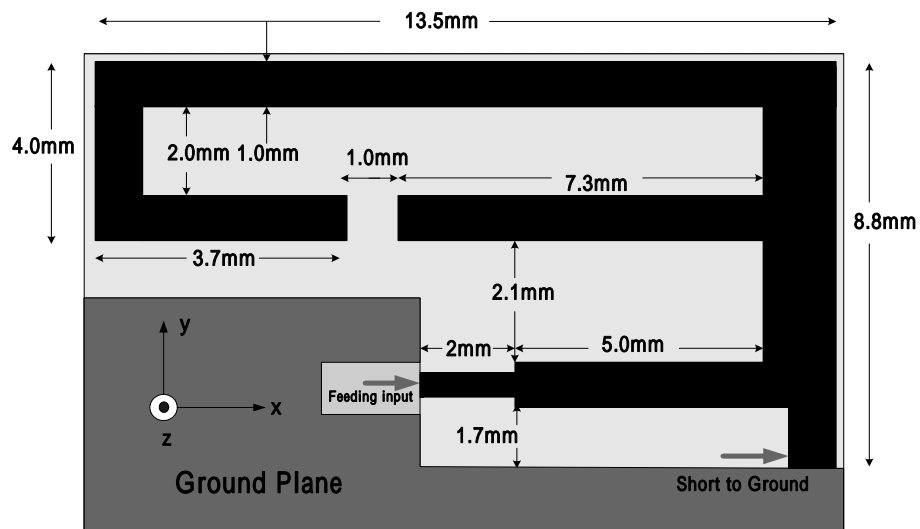


Figure 3-11: Geometry of dual-band monopole antenna with another design. (a) Detail geometry and dimensions (b) On parylene substrate (c) Fabricated on a Bluetooth dongle.

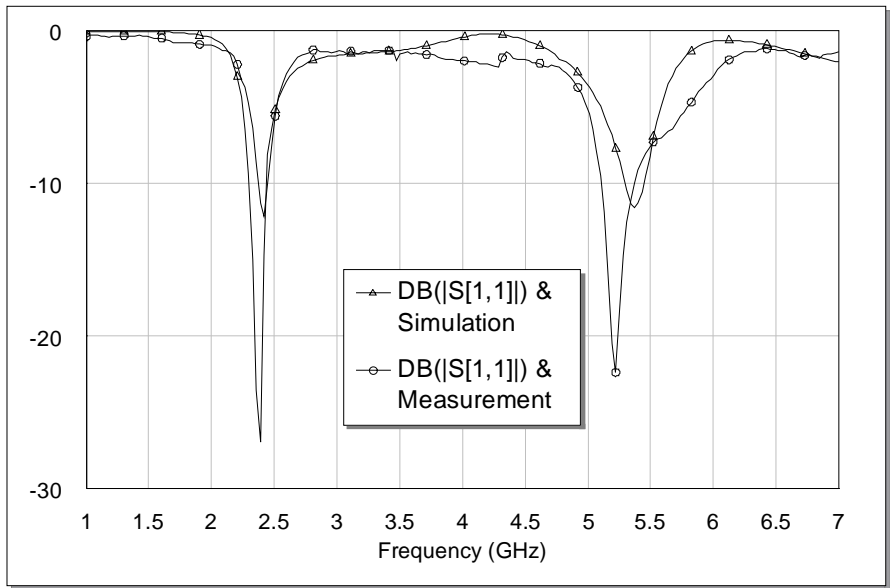
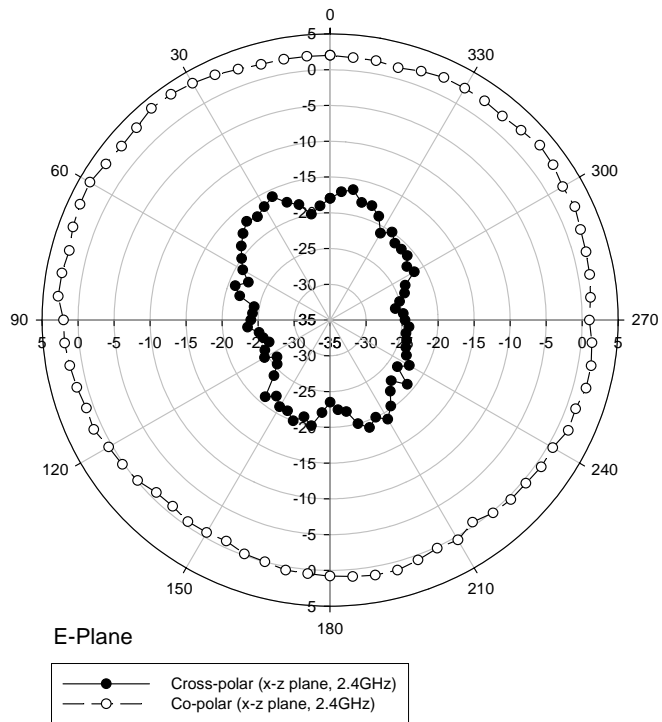
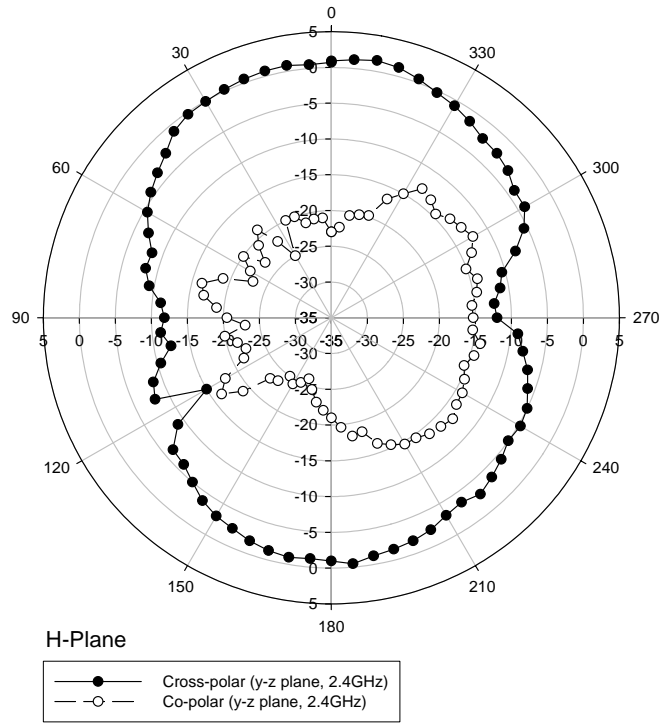


Figure 3-12: Measured and simulated return loss for the dual-band monopole antenna with another design (2.4 and 5.2 GHz for Bluetooth and WLAN).

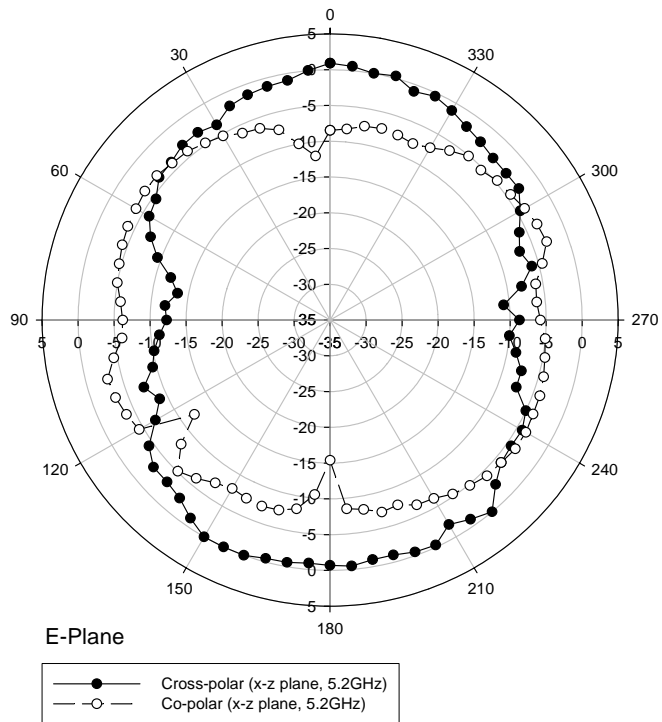


(a)

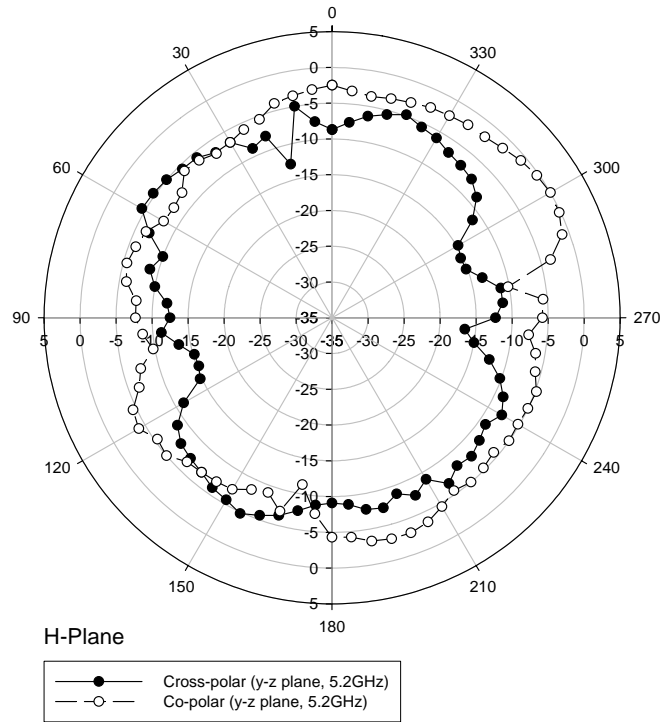


(b)

Figure 3-13: Measured x-z and y-z plane radiation patterns at 2.4 GHz of the antenna with G-shape design.



(a)



(b)

Figure 3-14: Measured x-z and y-z plane radiation patterns at 5.2 GHz of the antenna with G-shape design.



Figure 3-15: RFID antennas with different dimensions were fabricated on a flexible parylene membrane.